# PARAMETER DETERMINATION OF A SINGLE-PHASE SYNCHRONOUS RELUCTANCE MOTOR FROM TESTS

By

**Emeka S. Obe and Linus U. Anih**
*Department of Electrical Engineering,*
*University of Nigeria*
*Nsukka*

## ABSTRACT

*A test procedure for determining the parameters of a single-phase synchronous reluctance motor is presented. By applying the principle of harmonic balance, a set of non-linear simultaneous equations, capable of yielding all the parameters of single-phase reluctance motor from test results are obtained. Values of axes inductances obtained from measurements are validated by finite element (FE) simulations and it is observed that there is a correlation between the measured and simulation results.*

**Index terms**: flux linkages, magnetizing inductance, electromagnetic torque, saturation effects, finite element.

## 1. Introduction

Two popular methods of measuring the parameters of single phase machines (the single phase and the "two-phase" methods) appear frequently in literature [1-6, 8-10] (and the references contained therein). Single phase methods [8, 10] entail a blocked rotor and no load tests performed with main and auxiliary windings excited one at a time and measurements taken. Ojo, et al [3] adopted this method and termed it "synchronous tests". Specifically, [8] reviewed the methods of measurement from the point of view of on-line and off-line methods, and used an on-line method to measure the parameters. The 2-phase methods, [1, 3, 4] are similar to the single phase method except that for the later, both windings are excited at the same time and measurements are taken simultaneously with the requirement that the currents in the two windings be $90^{\circ}$ out of phase and their magnitudes in inverse proportion to the turns ratio. Most publications on parameter determination of single phase motors focus directly on induction motors. Single phase reluctance motors have received very little attention [5] in that regard, yet it presents a better alternative to permanent magnet machines due to its cheapness and robustness. The motivation for this research derives from the facts that:

(a) single-phase reluctance motors are used in applications where precision is required, and therefore, accurate methods of determining the parameters are required.

(b) conventional methods of determining the parameters of synchronous and induction motors cannot be used because single phase reluctance motors have been shown to exhibit optimal performance if a run capacitor is present in the auxiliary winding circuit [1, 4]. This capacitor will influence the results if the usual methods are used.

(c) The technique adopted in this paper eliminates friction and windage losses present in no-load tests.

The equations suitable for calculating the parameters are first derived, the experimental procedure presented and the results confirmed by FE simulations. Saturation effects are included in the FE simulations to make the results comparable.

## 2. Analysis

The d-q equations for a single phase reluctance motor operating without a running capacitor in the rotor reference frame are [1]:

$V_{qs} = r_{aa}I_{qs} + r_{ab}I'_{ds} + \omega_r\lambda'_{ds} + p\lambda_{qs}$ ......(1)

$V_{ds} = r_{bb}'I'_{ds} + r_{ab}I_{qs} + p\lambda'_{ds} - \omega_r\lambda'_{qs}$ ....(2)

$V_{qr} = r_{qr}'I'_{qr} + p\lambda'_{qr}$ .......................(3)

$V_{dr} = r'_{dr}I'_{dr} + p\lambda'_{dr}$ .......................(4)

The electromagnetic torque is:

$T_e = \frac{1}{2} P.(I_{qs}\lambda_{ds}' - I_{ds}'\lambda_{qs})$ .................(5)

where,

$$\begin{bmatrix} \lambda_{qs} \\ \lambda_{qr}' \\ \lambda_{ds}' \\ \lambda_{dr}' \end{bmatrix} = \begin{bmatrix} L_{qs} & L_{mq} & 0 & 0 \\ L_{mq} & L_{qr}' & 0 & 0 \\ 0 & 0 & L_{ds} & L_{md} \\ 0 & 0 & L_{md} & L_{dr}' \end{bmatrix} \begin{bmatrix} I_{qs} \\ I'_{qr} \\ I'_{ds} \\ I'_{dr} \end{bmatrix}$$

and,

$L_{qs} = L_{lqs} + L_{mq}$, $L_{qr}' = L_{lqr}' + L_{mq}$

$L_{ds} = L_{lds} + L_{md}$, $L_{dr}' = L_{ldr}' + L_{md}$

$r_{aa} = \frac{1}{2}(r_{as} + r_{bs}') + \frac{1}{2}(r_{as} - r_{bs}')\cos 2P\theta_r$

$r_{ab} = \frac{1}{2}(r_{as} - r_{bs}')\sin 2P\theta_r$

$r_{bb} = \frac{1}{2}(r_{as} + r_{bs}') - \frac{1}{2}(r_{as} - r_{bs}')\cos 2P\theta_r$

$r_{bs}' = r_{bs}/k_{ab}^2$, $r_{dr}' = r_{br}k_{br}^2$, $r_{qr}' = r_{ar}k_{ar}^2$

$$\theta_r = \frac{1}{P}\int_0^t \omega_r t + \delta_o ,$$

P is number of poles, $\omega_r$ is the rotor speed. $\delta_o$ is the initial rotor angle. The subscripts s and r represents stator and rotor quantities respectively. The transformation ratios are:

$$k_{ab} = \frac{N_{BS}}{N_{AS}}, k_{ar} = \frac{N_{AS}}{N_{AR}} \text{ and } k_{br} = \frac{N_{AS}}{N_{BR}}$$

The primed quantities are the quantities referred to the main stator winding. The effective turns per pole for the two rotor windings are $N_{AR}$ and $N_{BR}$. Other parameters are as shown in the equivalent circuit of Fig. 1 which is derived from equations (1) to (4).

These equations are suitable for transient and dynamic predictions but not sufficient to yield machine parameter values and/or their influence on transient torque components and their magnitudes. This paper sets forth to obtain these information by assuming a constant instantaneous speed (quasi-steady-state condition) and applying the harmonic balance technique [6, 7] to equations (1) to (5). By applying phasor analysis to non-linear differential equations, harmonic balance decouples the state variables into a combination of sinusoids (in a manner similar to Fourier series) to form simple linear simultaneous equations, each representing different harmonic components. As many harmonics as desired can be considered; the solution found by equating corresponding coefficients of the sinusoids. The advantage of this decoupling is that it offers the state variables and torques in component parts in a form amenable to control. This approach has been of great utility especially in systems with unbalanced operation and in understanding the contribution of each harmonic component to the overall system performance.

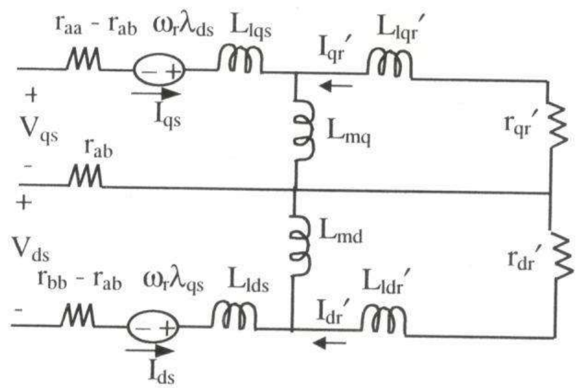


**Fig. 1: d-q Equivalent circuit**

The basic theorems guiding this technique are given in section 7. For generality, let the source voltages be:

$V_{aa}=V_a\cos(\omega_e t+\varepsilon_a)$and $V_{bb} = V_b\cos(\omega_e t+\varepsilon_b)$

The q- and d- axis voltages expressed in complex form are:

$$V_{qs} = \mathrm{Re}\left(V_{qs1}e^{j\theta_1} + V_{qs2}e^{j\theta_2}\right)$$
$$V_{ds} = \mathrm{Re}\left(V_{ds1}e^{j\theta_1} + V_{ds2}e^{j\theta_2}\right)$$

where, $\theta_1 = \theta_e + \theta_r$, $\theta_2 = \theta_e - \theta_r$,

$$V_{qs1} = \frac{1}{2}\left(V_a e^{j\sigma_a} + jV_b e^{j\sigma_b}\right)$$
$$V_{qs2} = \frac{1}{2}\left(V_a e^{j\eta_a} - jV_b e^{j\eta_b}\right)$$
$$V_{ds1} = \frac{1}{2}\left(jV_a e^{j\sigma_a} - V_b e^{j\sigma_b}\right)$$
$$V_{qs2} = \frac{1}{2}\left(-jV_a e^{j\eta_a} - V_b e^{j\eta_b}\right)$$

where $\sigma_a = \varepsilon_a+\delta_o$, $\eta_a = \varepsilon_a - \delta_o$, $\sigma_b = \varepsilon_b+\delta_o$ and $\eta_b = \varepsilon_b - \delta_o$.

Again, let the currents in the main and auxiliary windings be:

$I_{aa} = I_a\cos(\omega t+\varphi_a)$ and $I_{bb} = I_b\cos(\omega t+\varphi_b)$ respectively. The q- and d-components of current can also be found to be:

$$I_{qs1} = \frac{1}{2}(I_a + jI_b)e^{j\beta} \quad I_{qs2} = \frac{1}{2}(I_a - jI_b)e^{j\rho}$$
$$I_{ds1} = \frac{1}{2}(jI_a - I_b)e^{j\beta}$$
$$I_{ds2} = \frac{1}{2}(-jI_a - I_b)e^{j\rho}$$

where $\beta = \varphi_a + \delta_o$ and $\rho = \varphi_b - \delta_o$. $\varphi_a$ and $\varphi_b$ are the power factor angles of the main and auxiliary windings respectively.

Since a constant instantaneous speed is assumed, the d-q voltage equations are linear; suggesting that the flux linkages and currents have the same forms as the d- and q- axis voltages. That is:

$$I_{qs} = \mathrm{Re}\left(I_{qs1}e^{j\theta_1} + I_{qs2}e^{j\theta_2}\right)$$
$$I_{qr}' = \mathrm{Re}\left(I_{qr1}e^{j\theta_1} + I_{qr2}e^{j\theta_2}\right)$$
$$I_{dr}' = \mathrm{Re}\left(I_{dr1}e^{j\theta_1} + I_{dr2}e^{j\theta_2}\right)$$

$$\lambda_{qs} = \mathrm{Re}\left(\lambda_{qs1}e^{j\theta_1} + \lambda_{qs2}e^{j\theta_2}\right)$$
$$\lambda_{ds} = \mathrm{Re}\left(\lambda_{ds1}e^{j\theta_1} + \lambda_{ds2}e^{j\theta_2}\right)$$
$$\lambda_{qr} = \mathrm{Re}\left(\lambda_{qr1}e^{j\theta_1} + \lambda_{qr2}e^{j\theta_2}\right)$$
$$\lambda_{dr} = \mathrm{Re}\left(\lambda_{dr1}e^{j\theta_1} + \lambda_{dr2}e^{j\theta_2}\right)$$

If these are substituted into equations (1-4) and harmonic balance technique applied, we obtain:

$V_{qs1} = r_{aa}I_{qs1} + p\lambda_{qs1} + \omega_r\lambda_{ds1} + j(\omega_e+\omega_r)\ \lambda_{qs1}$ ...(6)

$V_{ds1} = r_{bb}I_{ds1} + p\lambda_{ds1} - \omega_r\lambda_{qs1} + j(\omega_e+\omega_r)\ \lambda_{ds1}$ .....(7)

$V_{qr1} = r_{qr}'I_{qr1} + p\lambda_{qr1} + j(\omega_e+\omega_r)\ \lambda_{qr1}$ ..(8)

$V_{dr1} = r_{dr}'I_{dr1} + p\lambda_{dr1} + j(\omega_e+\omega_r)\ \lambda_{dr1}$ ..(9)

$V_{qs2} = r_{aa}I_{qs2} + p\lambda_{qs2} + \omega_r\lambda_{ds2} + j(\omega_e-\omega_r)\ \lambda_{qs2}$...(10)

$V_{ds2} = r_{bb}I_{ds2} + p\lambda_{ds2} - \omega_r\lambda_{qs2} + j(\omega_e-\omega_r)\ \lambda_{ds2}$ ....(11)

$V_{qr2} = r_{qr}'I_{qr2} + p\lambda_{qr2} + j(\omega_e-\omega_r)\ \lambda_{qr2}$ ..........(12)

$V_{dr2} = r_{dr}'I_{dr2} + p\lambda_{dr2} + j(\omega_e-\omega_r)\ \lambda_{dr2}$ ...(13)

It is observed that the d-and q- voltages and currents each have two components rotating at angular frequencies of $\omega_e$-$\omega_r$ and $\omega_e$+$\omega_r$.

Similarly, the torque equation (5) will modify to:

$$T_e = \frac{P}{4}\mathrm{Re}\begin{pmatrix} T_0 + T_1e^{j2\theta_r} + T_2e^{j2\theta_e} \\ + T_3e^{j2(\theta_e+\theta_r)} + T_4e^{j2(\theta_e-\theta_r)} \end{pmatrix} \quad (14)$$

where

$T_0 = \lambda_{ds1}I_{qs1}^* + \lambda_{ds2}I_{qs2}^* - \lambda_{qs1}I_{ds1}^* - \lambda_{qs2}I_{ds2}^*$

$T_1 = \lambda_{ds1}I_{qs2} + \lambda_{ds2}I_{qs1} - \lambda_{qs1}I_{ds2} - \lambda_{qs2}I_{ds1}$

$T_2 = \lambda_{ds1}I_{qs2}^* - \lambda_{qs1}I_{ds2}^* + \lambda_{ds2}^*I_{qs1} - \lambda_{qs2}^*I_{ds1}$

$T_3 = \lambda_{ds1}I_{qs1} - \lambda_{qs1}I_{ds1}$,

and $T_4 = \lambda_{ds2}I_{qs2} - \lambda_{qs2}I_{ds2}$

State variables with * implies conjugates.

Hence apart from the average torque component, $T_0$, there are four additional torque components oscillating at speeds ($\omega_e$-$\omega_r$), ($\omega_e$+$\omega_r$), $2\omega_e$ and $2\omega_r$.

The average and pulsating torque equations are:

$$T_{AV} = \frac{P}{4}\mathrm{Re}(T_0 + T_4)$$

$$T_{puls} = \frac{P}{4}\mathrm{Re}(T_1 + T_2)e^{j2\theta_e} + T_3e^{j4\theta_e}$$

A more detailed study of these torque components and their influence in machine behaviour warrant a different study and are therefore not pursued further here.

### 3. Parameter determination

The machine used for this study is a commercial single-phase 1 hp, 115/230V, 60Hz reluctance motor made by Reliance Electric Industry Company. For the purpose of determination of machine parameters, all time varying state variables in equations (6) to (13) are set to zero. The dc test was used to measure $r_{as}$ and $r_{bs}$ from which the vector resistances, $r_{aa}$ and $r_{bb}$ were calculated. $r_{ab}$ is assumed to be equal to zero with negligible loss of accuracy. A variable voltage constant frequency source is then used to energize the motor (without a starting capacitor), the rotor will not move, hence $\omega_r = 0$. The voltage was then increased gradually from zero to a value at which the main winding current equals its rated value. By virtue of the short-circuited nature of the rotor cage bars, $V_{qr1}$, $V_{dr1}$, $V_{qr2}$ and $V_{dr2}$ are all equal to zero. Noting that $I_{ds1} = -jI_{qs1}$ and $I_{ds2} = jI_{qs2}$, equations (6) to (9) are manipulated to:

$$\frac{V_{qs1}}{I_{qs1}} = r_{aa} + j\omega_e L_{qs} + \frac{\omega_e^2 L_{mq}^2}{r_{qr} + j\omega_e L_{qr}}, \quad \ldots(14)$$

$$\frac{V_{ds1}}{I_{ds1}} = r_{bb} + j\omega_e L_{ds} + \frac{\omega_e^2 L_{md}^2}{r_{dr} + j\omega_e L_{dr}}, \quad \ldots(15)$$

If we assume that the magnetizing reactances $L_{mq}$ and $L_{md}$ are much greater than the leakage reactances, $L_{lqr}$, $L_{lqs}$, $L_{ldr}$ and $L_{lds}$, then, equations (14)+(15) gives:

$$\frac{1}{2}\left(\frac{V_{qs1}}{I_{qs1}} + \frac{V_{qs2}}{I_{qs2}}\right) = \left(\begin{matrix}(r_{aa} + r_{qr}) \\ + j\omega_e(L_{lqs} + L_{lqr})\end{matrix}\right) \ldots..(16)$$

Similar procedure on (10) to (13) also yields:

$$\frac{1}{2}\left(\frac{V_{ds1}}{I_{ds1}} + \frac{V_{ds2}}{I_{ds2}}\right) = \left(\begin{matrix}(r_{bb} + r_{dr}) \\ + j\omega_e(L_{lds} + L_{ldr})\end{matrix}\right) \ldots..(17)$$

Equations (16) and (17) are evident from the circuit of Fig. 1 if it is assumed that the shunt branches present infinite impedance as is usually assumed in blocked rotor tests for induction motors [2,10].

If we equate the real parts of (16) and (17), we obtain expressions that can be solved for values of $r_{dr}$ and $r_{qr}$ respectively. The q-axis leakage reactance, $L_{lqr}+L_{lqs}$ can be found by equating the imaginary parts of (16) while $L_{ldr}+L_{lds}$ results by equating the imaginary parts of (17). To determine the remaining parameters - $L_{md}$ and $L_{mq}$, the procedure is to drive the rotor of the reluctance motor at synchronous speed using a dc motor of higher horsepower. Driving the motor this way will eliminate the errors due to windage, friction and oscillatory torques that would occur if the conventional no-load tests are used. The voltage across the main (and auxiliary) windings was increased gradually from zero to rated value. Measurements on main winding current $I_a$ and power $P_a$, and auxiliary winding current $I_b$ and power $P_b$ were then taken for every step increase of input voltage. For this test, $\omega_r = \omega_e$. Applying this condition to equations (6) to (13) and proceeding as in the blocked rotor test, we have:

$$\frac{1}{2}\left(\frac{V_{qs1}}{I_{qs1}} + \frac{V_{qs2}}{I_{qs2}}\right) = \left(r_{aa} + j\omega(L_{ds} + L_{qs})\right) + \omega^2\left(\frac{2L_{mq}^2}{r_{qr} + j2\omega L_{qr}} + \frac{L_{md}^2}{r_{dr} + j2\omega L_{dr}}\right) \ldots\ldots(18)$$

$$\frac{1}{2}\left(\frac{V_{dsl}}{I_{qsl}} + \frac{V_{ds2}}{I_{qs2}}\right) = \left(jr_{bb} - \omega(L_{ds} + L_{qs})\right) + j\omega^2\left(\frac{L_{mq}^2}{r_{qr} + j2\omega L_{qr}} + \frac{2L_{md}^2}{r_{dr} + j2\omega L_{dr}}\right) \ldots\ldots(19)$$

$L_{md}$ and $L_{mq}$ can now be computed from simultaneous solution of (18) and (19) for every step increase in input voltage. Plots of measured and computed $L_{md}$ and $L_{mq}$ versus input voltage is shown in Fig. 2. The measured values are:

$r_{as} = 2.0\Omega$, $r_{bs} = 2.8\Omega$, $k_{ab} = 1.8$, $k_{ar} = 2.2$,

$k_{br} = 2.2$ $l_{lqs} = 0.012H$, $l_{lds} = 0l012H$,

$l_{lqr} = 0.024H$, $l_{ldr} = 0.019H$, $r_{qr} = 1.1\Omega$,

$rdr = 1.21\Omega$

## 4. Finite element simulations

One accurate computational tool that has offered a way of determining the parameters of electrical machines is the finite element analysis. Using this method, one can safely "excite" the machines with very high voltage and study its behavior without actually having to risk the physical machine. To accomplish this, accurate information on the winding distribution, number of slots, number of turns of coils and every other design detail of the machine is needed. To account for saturation effects the experimental variation of $L_{md}$ and $L_{mq}$ obtained by second order curve-fit of Fig. 2 is used in the FE simulations. The expressions thus obtained are:

$$L_{md}=318.76V_m^2+128.74V_m+176.47 \quad ..(20)$$

and

$$L_{mq}= 525.93V_m^2+351.70V_m+0.63 \quad ......(21)$$

where $V_m = V_{aa} = V_{bb}$

For the machine under study, the clock diagram is as shown in Fig. 3, and the total current in one-half of the machine periphery is as shown in Table 1.

The flux lines and magnetic flux density plots obtained for a particular value of input voltage (115V) are shown in Fig. 4

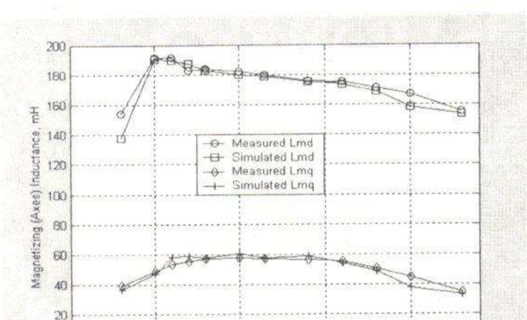


**Fig. 2: Measured and simulated d- and q-axis magnetizing inductances as a function of airgap flux linkage**

**Table 1: Total slot current used in the computation of the finite element analysis**

| Slot | Number of conductors | | Total current in slot |
|---|---|---|---|
| | Main winding | Auxiliary winding | |
| 1 | 12+ | 2+ | 74.8240 |
| 2 | 26+ | 0 | 152.1780 |
| 3 | 28+ | 0 | 163.8840 |
| 4 | 28+ | 0 | 163.8840 |
| 5 | 26+ | 0 | 152.1780 |
| 6 | 12+ | 2+ | 74.8240 |
| 7 | 0 | 13+ | 29.8220 |
| 8 | 0 | 0 | 0.0000 |
| 9 | 0 | 13- | -29.8220 |
| 10 | 12- | 2- | -74.8240 |
| 11 | 26- | 0 | -152.1780 |
| 12 | 28- | 0 | -163.8840 |
| 13 | 28- | 0 | -163.8840 |
| 14 | 26- | 0 | -152.1780 |
| 15 | 12- | 2- | -74.8240 |
| 16 | 0 | 13- | -29.8220 |
| 17 | 0 | 0 | 0.0000 |
| 18 | 0 | 13+ | 29.8220 |

+ slot in which current enters

- slot in which current leaves

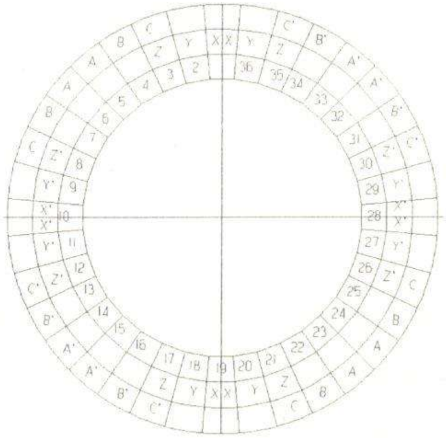

(A, B, C, A′, B′, C′ belong to the main winding while X, Y, Z, X′, Y′ and Z′ belong to the auxiliary winding)

Fig. 3: Clock diagram

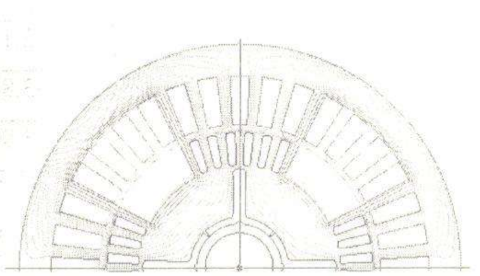

(a) Flux lines

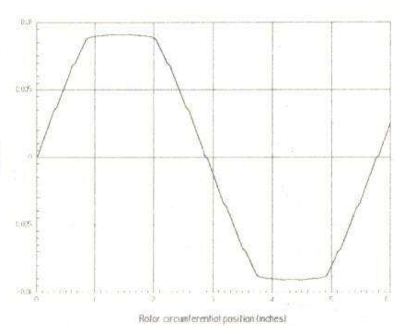

(b) Magnitude of airgap flux density

**Fig. 4: FE simulation plots**

Using spectral analysis, the fundamental component of flux density in Fig. 4 can be extracted and used to calculate the $L_{md}$ and $L_{mq}$ from the following equations [5]:

$$L_{md} = \frac{1}{I_{ds}}\left(\frac{K_1 N_1}{N_C}\right)\left(\frac{2}{\pi}B_{gld}\right)\tau_p l_e \text{......(22)}$$

$$L_{mq} = \frac{1}{I_{qs}}\left(\frac{K_1 N_1}{N_C}\right)\left(\frac{2}{\pi}B_{glq}\right)\tau_p l_e \text{......(23)}$$

where, $K_1$ is the winding factor, $N_1$ is the number of turns, $N_c$ number of circuit in parallel, $B_{gld}$ and $B_{glq}$ are the fundamental components of the airgap flux density in the d- and q-axes respectively, $\tau_p$ is the pole pitch, $l_e$ is the effective core length. The results of these computations together with experimental values are shown in Table 2.

**Table 2: Measured and simulated values of $L_{md}$ and $L_{mq}$ (input voltage is $V_a = V_b$)**

| Voltage (V) | $L_{md}$ (mH) | | $L_{mq}$ (mH) | |
|---|---|---|---|---|
| | Measured | FE | Measured | FE |
| 30 | 154.0 | 137.5 | 39.2 | 36.5 |
| 50 | 191.5 | 190.4 | 48.6 | 47.1 |
| 60 | 191.5 | 190.0 | 53.5 | 58.1 |
| 70 | 183.0 | 187.5 | 55.5 | 58.7 |
| 80 | 184.0 | 183.0 | 57.0 | 57.7 |
| 100 | 182.2 | 180.0 | 57.5 | 60.8 |
| 115 | 180.0 | 178.5 | 57.0 | 57.6 |
| 140 | 176.4 | 175.3 | 56.5 | 58.8 |
| 160 | 175.0 | 173.4 | 55.0 | 54.2 |
| 180 | 171.0 | 168.8 | 50.5 | 48.9 |
| 200 | 167.1 | 158.3 | 44.5 | 37.7 |
| 230 | 155.0 | 153.4 | 35.0 | 32.8 |

## 5. Conclusions

Methods of measuring parameters of single phase motors were reviewed and a technique that is capable of eliminating all the errors inherent in no-load tests were subjected to reluctance type machine. Results obtained from these measurements were compared with FE simulations and a low degree of discrepancy observed.

### 6. References

[1] E. S. Obe "Analysis of single-phase line-start ac motors". An unpublished research report submitted to the Center of Electric Power Tennessee Tech University, USA. August 12, 2004.

[2] C. van der Merwe and F. S. van de Merwe, "A study of the methods to measure the parameters of single-phase induction motors", *IEEE Trans. on Energy Conversion*, Vol. 10, No. 2, June 1995, pp.248-253

[3] O. Ojo, O. Omozusi, M. Omogui and A. A. Jimoh, "Parameter Estimation of single-phase induction machines", Conference record of 36th IAS Annual meeting, Sept 30 to Oct 4, 2001 Chicago, IL. p.2280-2287,

[4] O. Ojo, A. Ginart, O. Omozusi, A. A. Jimoh, "Modeling and analysis of a single-phase synchronous reluctance machine including saturation effect", Conference Record of Industry Applications Society Annual meeting, Louisiana October 5-9, 1997. pp.

[5] T. Matsuo and T. A. Lipo, "Rotor design optimization of synchronous reluctance machine" *IEEE Trans. on Energy Conversion*, Vol. 9, N. 2, June 1994, pp.359-365.

[6] A. H. Nayfeh and B. Balachanran, *Applied Nonlinear Dynamics* John Wiley and Sons, Inc, 1995

[7] J. Chen and P. Famouri, "Single-phase self-excited reluctance generator, part I: Steady-State Analysis" *Electric Power Components and Systems*, **31**, pp.129-147, 2003.

[8] A. Kilthau and J. M. Pacas, "Parameter-Measurement and control of synchronous reluctance machine including Cross saturation" Conference Record of the 36thIndustry Applications Society Annual Meeting, Sept 30 to Oct 4, 2001 Chicago, IL. p. 2302-2309.

[9] R. E. Fairbairn and R. G. Harley, "On-line Measurement of synchronous machine parameters" *IEEE Trans. on Industry Applications*, Vol. 28, No. 3, May/June 1992. p. 639-645.

[10] Suhr, F. W "Towards an accurate evaluation of single-phase induction motor constants" *Trans AIEE* Part 3, power Apparatus and Systems, Vol 71, January 1952, p. 221-227

## 7. Appendix: Harmonic balance technique [6]

Since many circuits generally operate in the sinusoidal steady state and it is known that if the response of a linear time-invariant circuit to a sinusoidal input of any frequency is known, then effectively, its response to any signal can be calculated, the harmonic balance technique finds applications in electric motor analysis. The method is efficient is supported by the following three theorems:

***(a) Uniqueness***: Two sinusoids are equal if and only if they are represented by the same phasor; symbolically, for all t,

$$\text{Re}[Ae^{jwt}] = \text{Re}[Be^{jwt}\} \Leftrightarrow A = B$$

***(b) Linearity:*** The phasor represented by a linear combination of sinusoids (with real coefficients) is equal to the same linear combinations of the phasor representing the individual sinusoids.

Symbolically, let the sinusoids:

$x_1(t) = \text{Re}[A_1e^{j\omega t}]$ and $x_2(t) = \text{Re}[A_2e^{j\omega t}]$

Let $a_1$ and $a_2$ be any two real numbers; then the sinusoid $a_1x_1(t) + a_2x_2(t)$ is represented by the phasor: $a_1A_1 + a_2A_2$.

***(c) Differentiation:*** *A* is the phasor of a given sinusoid $A_m\cos(\omega t+\theta)$ if and only if $j\omega A$ is the phasor of its derivative,

$\frac{d}{dt}[A_m \cos(\omega t + \theta)]$. Symbolically,

$$\text{Re}(j\omega Ae^{j\omega t}) = \frac{d}{dt}\left[\text{Re}(A_m e^{j\omega t})\right].$$

This indicates that the linear operators Re and $\frac{d}{dt}$ commute. i.e.

$$\text{Re}\left[\frac{d}{dt}\left(A_m e^{j\omega t}\right)\right] = \text{Re}\left[j\omega A_m e^{j\omega t}\right]$$
$$= \frac{d}{dt}\left(\text{Re}\left(A_m e^{j\omega t}\right)\right)$$

## 8.0 Appreciation:

The laboratory privileges granted by Dr. J. Ojo of Center for Electric Power Tennessee Technological University, Cookeville USA are highly appreciated.